

C. S. GROMMÉ

E. H. McKEE

M. C. BLAKE, JR.

*U.S. Geological Survey, Menlo Park, California 94025*

# Paleomagnetic Correlations and Potassium-Argon Dating of Middle Tertiary Ash-Flow Sheets in the Eastern Great Basin, Nevada and Utah

## ABSTRACT

Directions of natural remanent magnetization are used to identify and correlate individual cooling units in the middle Tertiary ash-flow province in central and eastern Nevada and western Utah. Potassium-argon dating indicates that the minimum time between eruptions of individual but genetically related ash-flow cooling units is on the order of 0.8 m.y. As this interval is long in comparison with the secular variation of the direction of the geomagnetic field, in a given volcanic province the direction of natural thermoremanent magnetization is a unique characteristic of each cooling unit. Ash-flow sheets investigated include the Stone Cabin Formation, the tuff of Pancake Summit, the Windous Butte Formation, the Needles Range Formation, the Bates Mountain Tuff, and the tuff of Clipper Gap, of Oligocene to early Miocene age. The original areas of individual ash-flow cooling units are as great as 8,000 km<sup>2</sup>; the volumes, 1,300 km<sup>3</sup>. The paleomagnetic correlations, made over distances up to 200 km, confirm most of the previously made lithologic correlations and allow more accurate delineation of single cooling units. These correlations are particularly useful in those parts of the Basin and Range province where the Tertiary stratigraphic section consists mainly of ash-flow sheets, and the outcrops are confined to mountain ranges that are separated by alluvium-filled valleys.

## INTRODUCTION

The great regional extent of Tertiary ash-flow sheets in the eastern Great Basin of Nevada and Utah was first clearly documented by J. H. Mackin in 1960. Referring to rocks in western Utah, he stated that "some individual ignim-

brites are hundreds of feet in thickness over an area measured in many thousands of square miles" and speculated that the eruption of the hundreds of cubic miles of gas-filled magma required to form such ignimbrites took place over a very short period of time. An extensive investigation made by Cook (1965) of the Tertiary ignimbrite stratigraphy in eastern Nevada contributed evidence supporting Mackin's ideas on the great lateral extent and volume of ash from such eruptions. Cook (1965) used megascopic and microscopic criteria as well as stratigraphic relations to correlate individual ash flows over distances as great as 100 mi or more. These criteria include total amount and relative proportions of phenocrysts; proportions of crystal, lithic, and vitric components; nature and degree of welding and color; and position in the stratigraphic sequence.

Recent geologic mapping in central and eastern Nevada has extended and added to the stratigraphy established by Cook (McKee and Stewart, 1971; Stewart and McKee, 1970; Hose and Blake, 1970; Nolan and others, in prep.). Because the ash-flow sheets constitute such an important element of the Tertiary rocks in much of the Great Basin, they are the most useful units for reconstructing the Tertiary geologic history. In addition, they represent volcanic eruptions of such widespread nature that it is desirable to verify the lithologic correlations of the individual ash-flow sheets by an independent method. During the course of a paleomagnetic investigation of middle Tertiary volcanic rocks in the Great Basin (Grommé and McKee, 1971) it became evident that the directions of natural remanent magnetization (NRM) in welded ash-flow sheets could provide a unique means of correlating exposures of



tuff sheets in a stratigraphic sequence could be distinguished by variations in their magnetic properties. He was the first to suggest that relative time intervals between successive eruptions might be estimated from differences in NRM directions resulting from secular variation of the geomagnetic field and that magnetic properties might be used to determine the lateral extent of individual tuff sheets. In their investigation of the Thirsty Canyon Tuff of southern Nevada, Noble and others (1968) used the directions of NRM to distinguish and identify the Rocket Wash Member and the Spearhead Member, lithologically similar ash flows separated by a complete cooling break.

A more detailed and complete paleomagnetic study of a single Pleistocene ash-flow sheet, the Bishop Tuff in eastern California, was made by Dalrymple and others (1965). They found that the directions of NRM were essentially parallel throughout the major part of the tuff, over a lateral distance of 60 km and a vertical thickness of 170 m, and that NRM directions within xenolithic inclusions were parallel to that of the enclosing tuff. Several important implications result from this: (1) As Dalrymple and others (1965) concluded, although the Bishop Tuff is composed of a number of separate members (Gilbert, 1938), the uniformity of NRM directions indicates that their eruption and cooling occurred over a short period of time relative to geomagnetic secular variation; that is, within a few centuries or less. (2) The temperature of the tuff during emplacement and compaction was sufficiently high to impart a new magnetization to the xenolithic inclusions; this temperature must have been greater than the Curie temperatures of the inclusions and therefore probably greater than 580° C. (3) The horizontal planar fabric that is prominent in much of the tuff and is the result of compaction and welding might be expected to cause significant systematic deflection of the

NRM, either because of anisotropy of magnetic susceptibility (Fuller, 1963) or because of rotation of already magnetized material during the final stages of compaction and welding. The uniformity of NRM directions throughout the variably welded tuff and in the inclusions shows that such a systematic deflection did not occur. Because the Bishop Tuff is a typical example of a welded ash-flow sheet, these conclusions will be assumed to hold in general.

The measured Curie temperatures of the welded ash-flow sheets to be discussed below range from 570° to 630° C, whereas estimates of temperatures of welding range from 580° to 750° C or perhaps as great as 900° C (Ross and Smith, 1961). Thus while welding and concomitant plastic flow below the Curie temperature are not entirely ruled out, the fact that most thermoremanent magnetization in volcanic rocks is acquired over a range of temperature of 100° to 200° C or more below the Curie temperature (Nagata, 1961) implies that essentially all the NRM in these ash-flow sheets is acquired after welding is complete.

In contrast to the Bishop Tuff, an ash-flow sheet in which the NRM directions are not everywhere parallel has been investigated by Gose (1970); this is the Swett ignimbrite of Cook (1965). In a detailed study of a single 55-m thick exposure, Gose found both abrupt and gradual changes in NRM direction relative to vertical position in the ash flow. The total angular variation amounted to more than 60° and was tentatively interpreted to result from reheating by the overlying ash flow. It appears that this variation in NRM direction is unusual, because although many of the ash-flow sheets discussed below are overlain by later ones, we have found each of them to have uniform directions of magnetization, vertically as well as laterally.

### Precision of NRM Measurement

Standard methods were used in the collection

TABLE 1. APPROXIMATE DIMENSIONS AND THICKNESS RATIOS OF ASH-FLOW SHEETS

|                                     | Maximum lateral extent, km | Area km <sup>2</sup> | Volume km <sup>3</sup> | Thickness ratio |         |
|-------------------------------------|----------------------------|----------------------|------------------------|-----------------|---------|
|                                     |                            |                      |                        | average         | maximum |
| Tuff of Clipper Gap                 | 185                        | 6,300                | 190                    | 2,600           | 6,100   |
| Bates Mountain Tuff, unit D         | 220                        | 8,200                | 500                    | 1,500           | 3,600   |
| Windous Butte Formation             | 150                        | 8,200                | 1,300                  | 570             | 950     |
| Tuff of Pancake Summit              | 120                        | 5,400                | 750                    | 530             | 860     |
| Stone Cabin Formation, upper member | 100                        | 2,000                | 350                    | 250             | 570     |

Note: Thickness ratios are calculated as follows: Average thickness ratio =  $A^{3/2}/V$ , maximum thickness ratio =  $D/T$ , where  $T$  = average measured thickness,  $D$  = maximum lateral extent,  $A$  = area, and  $V$  = volume.

of oriented samples, measurement of NRM, and removal of spurious magnetizations. Geographically oriented cores collected at intervals of about 10 cm or more were obtained for several meters along the outcrops with a portable drill (see Doell and Cox, 1967a). The number of cores taken at each outcrop ranged from four to eighteen, usually ten. NRM directions in one specimen from each core were measured with a spinner magnetometer (Doell and Cox, 1965, 1967b), and secondary components of NRM were selectively removed by alternating field demagnetization using the equipment described by Doell and Cox (1967c).

For most outcrops, the directions of NRM were greatly scattered when first measured, probably owing to remagnetization by lightning currents (Cox, 1961; Graham, 1961). Alternating-field (a.f.) demagnetization has proved extremely successful in removing the secondary magnetizations, as illustrated in Figure 2. For a number of sites, the secondary magnetization could not be completely removed from one or more individual specimens; such specimens were omitted from the data analysis. The rationale and criteria for rejection of individual specimens have been discussed by Doell (1970) and by Grommé and others (1971). In the present work one or more specimens from 13 sites (of a total of 58 sites) were rejected; these specimens had mean NRM directions more than three root-mean-square angular dispersions away from the mean direction. In no case were more than half the specimens rejected, and the number was usually one or two. At only 1 of the 58 sites was it not possible to recover accurately the original magnetization direction; this exception will be discussed below. In the remainder of this paper, the term NRM will be used to mean the remanent magnetization after a.f. demagnetization.

The parameter most commonly used to describe the internal precision of the determination of the mean remanent magnetization (RM) direction in a rock unit is  $\alpha_{95}$  (Fisher, 1953), the semiangle of the cone centered about the calculated mean direction within which there is 95 percent probability that the true mean of the observed directions lies. For these ash-flow sheets the logarithmic mean of all values of  $\alpha_{95}$  is  $3.0^\circ$  after demagnetization. This precision is high compared with the uncertainties in compensating for structural deformation, to be discussed in the next section. But assuming the

structural uncertainties to be negligible, the precision of NRM measurement is sufficiently high to allow the possibility of distinguishing rocks erupted a few centuries apart.

### Correction for Tectonic Deformation

The greatest source of error in inferring the ancient magnetic field directions from the present NRM directions in these ash-flow sheets is the uncertainty in making exact corrections for tectonic deformation. Measured structural dips in the cooling units range from  $0^\circ$  to  $48^\circ$ , averaging  $17^\circ$ . The attitudes of some tuff outcrops could be determined from underlying sedimentary rocks, but usually it was necessary to use the planar tops of the ash-flow cooling units themselves. Ross and Smith (1961) have pointed out that the tops of undeformed ash-flow sheets are uniform and nearly horizontal surfaces even though they may have been erupted onto an irregular surface. In the

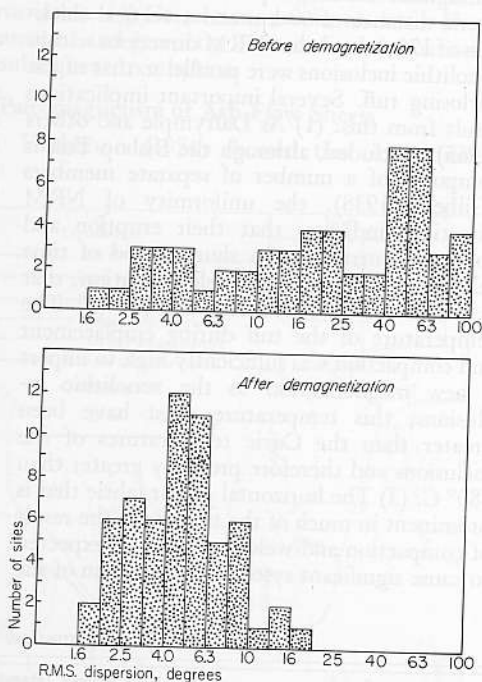


Figure 2. Effectiveness of alternating-field demagnetization in removing randomly directed secondary magnetizations. R.M.S. dispersion is the root-mean-square angular dispersion about the mean remanent magnetization direction for each site. Total number of sites is 57, average number of specimens at each site is 9, and peak demagnetizing fields range from 50 to 400 oersteds.

case of Oligocene and Miocene ash-flow sheets such as those studied in east-central Nevada, the planar surface most prominent on any outcrop is the top of the densely welded zone and not the original top of the deposit, which usually has been modified by later erosion. It is reasonable to assume that in most instances the two surfaces were nearly parallel. The error in dip measurement is no greater than  $\pm 5^\circ$  and usually of the order of  $\pm 2^\circ$ ; the error in strike measurement depends on the amount of dip, being of the order of  $\pm 5^\circ$  for a dip around  $20^\circ$ .

The correction for deformation is made in the usual way by "unfolding," that is, rotation of the bedding plane into the horizontal around a horizontal axis parallel to the strike. This is the only procedure that can be used in the absence of information other than dip and strike of the outcrop, and is justified because in the central Great Basin the structures resulting from deformation in later Tertiary time are mostly broad and uniform, consisting in general of large tilted fault blocks (Mackin, 1960). In one instance, to be discussed below, the use of this method leads to a serious error, but in general it has proven valid. It will be shown below that the root-mean-square angular deviations of mean NRM directions at all sites in the various single ash-flow sheets range from  $5.0^\circ$  to  $10.6^\circ$  after correction for deformation. These values can be compared with the logarithmic mean of the root-mean-square angular dispersions of specimen NRM directions at all sites (Fig. 2),  $5.5^\circ$ . As the uncertainty in determining the mean NRM direction of an outcrop in present-day coordinates is not as great as the uncertainty in transforming present-day coordinates to ancient coordinates, there is little need for increasing the precision of the magnetic measurements themselves. In short, the magnetic measurements are more precise than the structural corrections.

#### Probability of Different Rock Units Having the Same NRM Directions

If two occurrences of volcanic rocks that might be correlated on the basis of physical appearance and stratigraphic position, for example, two outcrops of welded tuff, turn out to have significantly different NRM directions, clearly they cannot both be products of the same eruption and cooling history and should not be correlated. The opposite assertion, that if two volcanic rocks of similar appearance and stratigraphic position have the same NRM

direction they are from the same eruption and hence may be correlated, requires additional justification. Cox (1971) has provided a statistical approach to this problem based on the assumption that the angular departures from the mean field direction due to secular variation over a long period of time have the probability distribution given by Fisher (1953). Given the NRM direction of cooling unit  $a$ , we wish to find the probability  $P_{a,b}$  of a cooling unit  $b$  of different age having an NRM direction not significantly different from that of cooling unit  $a$ . The expression obtained by Cox (1971) is

$$P_{a,b} = \frac{K}{2\pi} \left[ 1 - \cos(\alpha_a + \alpha_b) \right] \exp K \left[ \cos \delta_a - 1 \right]$$

where  $K$  is the precision parameter (Fisher, 1953) describing the amplitude of secular variation during the period of time under consideration,  $\delta_a$  is the angle between the NRM direction of cooling unit  $a$  and the mean field direction for that period of time, and  $\alpha_a$  and  $\alpha_b$  are the values of the 95 percent confidence radius  $\alpha_{95}$  for cooling units  $a$  and  $b$ , respectively.

For the interval from 22 to 37 m.y. ago, the mean paleomagnetic field direction in the Great Basin (irrespective of sign) was  $15.5^\circ$  west of north and  $54.1^\circ$  downward, and the dispersion of 67 independent, observed NRM directions about this mean is described by  $K = 10.0$  (Grommé and McKee, 1971). Of these 67 NRM directions, all representing different points in time, 31 are normal and 36 are reversed; hence there is approximately 50 percent probability of cooling unit  $b$  having the NRM polarity opposite from cooling unit  $a$ . Because in the model of Cox (1971) it was assumed that all the rocks under consideration were erupted during one polarity epoch, the probabilities  $P'_{a,b}$  that apply in the present case are one-half those calculated from the above expression.

For the purposes of these calculations, the reference NRM direction ( $a$ ) for each ash-flow cooling unit will be taken to be that at the type locality or reference locality specified when the unit was formally named. Values of  $\delta_a$  range from  $7^\circ$  to  $64^\circ$  and calculated probabilities  $P'_{a,b}$  from 0.005 to 0.00005. For small values of  $P$ , when more than two rocks are sampled, say units  $a$ ,  $b$ , and  $c$ , the probability  $P_{a,b,c}$  that

unit *b* or unit *c* will have the same NRM direction as unit *a* is

$$P_{a,b,c} = P_{a,b} + P_{a,c}.$$

In this study the number of localities sampled in each ash-flow in addition to the reference localities ranges from 3 to 8, and the corresponding overall probabilities  $P'_{a,b, \dots, n}$  range from 0.05 to 0.0002. Thus, in the least favorable case encountered in this study, there is only a 5 percent likelihood that one of the correlations is in error.

## CORRELATIONS OF COOLING UNITS

### Stone Cabin Formation

As named and described by Cook (1965), the type section of the Stone Cabin Formation is 8.2 mi southeast of Currant in sections 5 and 6, T. 9 N., R. 59 E., Nye County. It consists of two crystal-rich ash-flow sheets. The lower sheet has been renamed the Calloway Well Formation by Scott (1966) and Armstrong (1970), a usage which is not here adopted. The Stone Cabin Formation is the oldest ash-flow sequence in the eastern Great Basin Tertiary silicic volcanic province. Because the lower cooling unit is only very slightly welded, it was not sampled for paleomagnetic study. All the paleomagnetic samples were collected from four localities in the moderately to highly welded upper cooling unit. The NRM directions and associated parameters are given in Table 2, and the NRM directions and the geographic distribution of the upper cooling unit are shown in Figure 3. None of the four NRM directions coincides with any other but all are similar. Taking locality S3, the type section (Cook, 1965), as the reference direction, the value of the probability  $P'$  for three additional localities is only 0.0002; in other words, the NRM directions observed in the Stone Cabin Formation are distinctive. Note also that the difference in NRM directions between sites S3 and S4, where the geologic correlation is very good (Cook, 1965; Scott, 1966), is greater than the difference between sites S3 and S1, which are 70 km apart and where correlation is less certain (Fig. 3). At all four sites the physical aspect of the upper cooling unit is the same, as described by Cook (1965), and with the exception of site S3, where it overlies the lower cooling unit, the upper cooling unit is the oldest welded tuff in the Tertiary section. The unique NRM directions combined with

similar physical appearance and stratigraphic position make the correlation shown in Figure 3 virtually certain.

That the measured NRM directions in the upper cooling unit of the Stone Cabin Formation do not coincide is most likely due to uncertainty in correcting for deformation. This correction may be evaluated by comparing the dispersion of NRM directions before and after unfolding as in Table 3. The dispersion of the directions is reduced after unfolding (the precision parameter  $k$  increases) but the result is not statistically significant at the 95 percent confidence level according to the test of McElhinny (1964). The usefulness of this comparison is limited because the number of sites is small and all the sampled exposures dip in similar directions at low angles.

The upper cooling unit of the Stone Cabin Formation occurs, as shown in Figures 1 and 3, only in the Pancake, White Pine, and Grant Ranges and has a distribution quite different from that given by Cook (1965) for both cooling units. We have found the upper cooling unit to extend about 60 km farther northwest of the town of Currant than was shown by Cook, but the upper cooling unit is greatly restricted relative to the lower cooling unit northeast and southwest of sites S3 and S4 (Fig. 3). The maximum lateral extent of the upper cooling unit is 90 to 100 km, its area is roughly 2,000 km<sup>2</sup>, and its volume is on the order of 350 km<sup>3</sup>.

### Tuff of Pancake Summit

The Windous Butte Formation was shown by Cook (1965) as extending from its type section at the north end of the Grant Range (Fig. 1) nearly as far north as Eureka (lat. 39.5°) and westward at least to long. 116.5°. We have found that the northwestern exposures of welded tuff considered by Cook to be part of the Windous Butte Formation are instead part of an older lithologically similar crystal-rich ash-flow sheet which we will call the tuff of Pancake Summit. This unit, which greatly resembles the underlying Stone Cabin Formation as well as the overlying Windous Butte Formation is a crystal-rich rhyolitic ash-flow sheet, moderately to highly welded, that contains abundant prominent smoky quartz phenocrysts. Like the Stone Cabin and Windous Butte Formations, it contains approximately equal proportions of quartz, sanidine, and plagioclase phenocrysts with subordinate

mafic minerals (mostly biotite); phenocrysts make up about 30 percent of the rock (F. M. Byers, Jr., 1970, oral commun.). The most complete section of this tuff occurs at locality P5 (Fig. 4), approximately 2 km southwest of Pancake Summit in the northern Pancake Range, where the total thickness is 140 m. This corresponds to section PS of Cook (1965), who shows a similar thickness. At locality P4 in the Pancake Range (Fig. 4), the tuff of Pancake Summit overlies the Stone Cabin Formation (locality S1, Fig. 3) with a thin volcanic sandstone intervening, and 2 km northwest of Big Louis Spring in the Pancake Range (site P3, Fig. 4) it is overlain by the Windous Butte Formation (locality W3-W4).

The NRM directions at five sites and the minimum geographic extent of the tuff of Pancake Summit are shown in Figure 4: the magnetic data are in Table 1. After structural correction, the dispersion of the mean NRM directions is greatly decreased (Table 3) and, in fact, almost all the 95 percent confidence circles overlap one another. Although the NRM direction in the tuff of Pancake Summit is not very different from the mean geomagnetic field direction for that part of Tertiary time, taking P5 as the reference direction, the probability  $P'$  is only 0.05 that one of the other four sites is not the same age.

The maximum extent of the tuff of Pancake Summit in an east-west direction is 120 km (Fig. 4). The unit may extend farther southeast from the vicinity of site P3 than is indicated in Figure 4; the minimum area as shown is approximately 5,400 km<sup>2</sup>. The thickness of the ash-flow sheet is not well known, but taking the measurement of 140 m at Pancake Summit as typical, a minimum volume of 755 km<sup>3</sup> is suggested.

### Windous Butte Formation

The most prominent and easily recognized volcanic unit in the central part of the Great Basin is the Windous Butte Formation. It was named and defined by Cook (1965) for its occurrence about 1 mi south of Windous Butte, White Pine County. It consists of two crystal-rich ash-flow sheets, moderately to highly welded. In most places the two cooling units are welded together; this fact and the close petrographic similarity of the two units led Cook to suggest that they were separate phases of the same eruption.

Paleomagnetic data from 11 sites in the

upper and lower members are listed in Table 2. The NRM directions and the approximate geographic distribution are shown in Figure 5. At two localities, W3/W4 and W8/W9, where the lower and upper cooling units were sampled in juxtaposition, the NRM directions in the two members do not differ significantly. This supports Cook's suggestion that little time elapsed between the eruption of the two ash flows. At the other two localities where both cooling units were sampled (W6/W7 and W10/W11), the sites in the upper and lower members are separated by distances on the order of 500 m, and the fact that NRM directions in the two members differ significantly probably reflects errors in attitude measurement and structural correction. Combining results from the upper and lower cooling units and taking the total number of sites as 7, the formal probability  $P'$  that one of the correlations is in error is 0.01.

At two localities in the Windous Butte Formation, the NRM directions after structural correction do not coincide with those at the other sites. One of these is site W2, where the discrepancy is due to a large uncertainty in measurement of the attitude of the unit. The other locality, sites W10 and W11 at Shingle Spring in the Egan Range (Cook, 1965), presents a more difficult problem. As there is little doubt that the Windous Butte Formation has been correctly identified here, and the attitude measurements are relatively precise, we are forced to conclude that deformation in this vicinity has been more complex than simple tilting about a horizontal axis. The structure of this part of the Egan Range has been described in detail by Kellogg (1964), who showed that deformation had recurred throughout most of Cenozoic time and consisted mainly of repeated movement on various faults. In general, it appears that deformation during later Cenozoic time was more extensive in the Grant and Egan Ranges around latitude 38.5° N. (the areas around localities W5/W7 and W10/W11 in Fig. 5) than elsewhere in the area of this investigation.

If sites W2, W10, and W11 are omitted from the calculation, NRM directions at the remaining eight sites in the Windous Butte Formation converge significantly when the structural correction is made (Table 3). Although, like the tuff of Pancake Summit, the Windous Butte Formation is reversely magnetized, the NRM directions in these two

TABLE 2. MEAN DIRECTIONS OF NATURAL REMANENT MAGNETIZATION AT ALL SITES, AFTER PARTIAL ALTERNATING-FIELD DEMAGNETIZATION

| Site no.                   | Lat.  | Long.  | N  | R       | k     | $\alpha_{95}$ | I     | D     | H   | Remarks             |
|----------------------------|-------|--------|----|---------|-------|---------------|-------|-------|-----|---------------------|
| <u>Tuff of Clipper Gap</u> |       |        |    |         |       |               |       |       |     |                     |
| C 1 {20}                   | 39.22 | 243.15 | 12 | 11.9499 | 220   | 2.9           | 8.3   | 152.7 | 200 | type locality       |
| C 2                        | 39.36 | 243.39 | 7  | 6.9785  | 279   | 3.6           | -0.5  | 153.4 | 50  |                     |
| C 3                        | 39.06 | 243.49 | 4  | 3.9844  | 192   | 6.7           | -8.1  | 161.8 | 400 |                     |
| C 4                        | 39.38 | 244.25 | 10 | 9.9717  | 318   | 2.7           | -6.8  | 160.7 | 400 |                     |
| C 5                        | 39.52 | 245.70 | 10 | 9.9492  | 177   | 3.6           | 0.6   | 157.8 | 200 |                     |
| C 6                        | 38.32 | 243.16 | 7  | 6.9407  | 101   | 6.0           | 1.7   | 165.6 | 200 |                     |
| <u>Bates Mountain Tuff</u> |       |        |    |         |       |               |       |       |     |                     |
| B 1                        |       |        | 10 | 9.9606  | 228   | 3.2           | -67.7 | 146.1 | 200 | tuff A              |
| B 2                        |       |        | 10 | 9.9784  | 417   | 2.4           | 48.7  | 18.1  | 100 | tuff B              |
| B 3                        | 39.95 | 242.86 | 8  | 7.9913  | 805   | 2.0           | -38.6 | 201.0 | 100 | tuff C              |
| B 4                        |       |        | 10 | 9.9860  | 643   | 1.9           | 56.5  | 349.6 | 200 | tuff D              |
| B 5                        |       |        | 8  | 7.9949  | 1,379 | 1.5           | -65.8 | 139.1 | 100 | tuff A              |
| B 6                        | 39.74 | 243.20 | 8  | 7.9804  | 357   | 2.9           | 44.5  | 16.2  | 50  | tuff B              |
| B 7                        |       |        | 6  | 5.9947  | 938   | 2.2           | 57.6  | 335.8 | 200 | tuff D              |
| B 8 {25}*                  | 39.57 | 243.36 | 10 | 9.9846  | 586   | 2.0           | -60.5 | 117.7 | 200 | tuff A              |
| B 9                        | 39.56 | 243.37 | 10 | 9.9900  | 902   | 1.6           | 47.1  | 346.0 | 200 | tuff D              |
| B 10 {16}                  |       |        | 14 | 13.9110 | 146   | 3.3           | 39.1  | 17.8  | 200 | tuff B              |
| B 11 {17}                  |       |        | 10 | 9.9925  | 1,203 | 1.4           | -41.4 | 202.2 | 200 | tuff C              |
| B 12 {18}                  | 39.21 | 243.15 | 10 | 9.9585  | 217   | 3.3           | -50.4 | 202.9 | 200 | tuff C <sup>1</sup> |
| B 13 {19}                  | 39.22 | 243.15 | 11 | 10.9223 | 129   | 4.0           | 57.1  | 330.2 | 400 | tuff D              |
| B 14                       | 39.06 | 243.49 | 6  | 5.9808  | 260   | 4.2           | 62.7  | 2.4   | 200 | tuff D              |
| B 15                       | 39.04 | 243.68 | 10 | 9.9826  | 517   | 2.1           | 59.1  | 339.6 | 200 | tuff D              |
| B 16                       | 39.38 | 244.25 | 4  | 3.9087  | 33    | 16.3          | 52.6  | 9.7   | 200 | underlies B17       |
| B 17                       |       |        | 8  | 7.9822  | 394   | 2.8           | 59.8  | 335.8 | 400 | tuff D              |
| B 18                       | 40.05 | 242.72 | 9  | 8.6546  | 23    | 10.9          | 50.4  | 1.0   | 400 | tuff B              |
| B 19                       |       |        | 8  | 7.9690  | 226   | 3.7           | 60.5  | 330.4 | 400 | tuff D              |
| <u>Biote-Rich Tuff</u>     |       |        |    |         |       |               |       |       |     |                     |
| N 1 {15}                   | 39.21 | 243.15 | 10 | 9.8865  | 79    | 5.5           | -70.0 | 162.7 | 400 |                     |
| N 2 {22}                   | 39.23 | 243.23 | 8  | 7.9186  | 86    | 6.0           | -69.0 | 240.0 | 200 |                     |
| N 3 {25}                   | 39.57 | 243.36 | 10 | 9.9524  | 189   | 3.5           | -53.5 | 123.6 | 100 |                     |
| N 4 {84}                   | 39.36 | 243.39 | 6  | 5.9933  | 742   | 2.5           | -48.8 | 256.9 | 200 |                     |
| N 5 {85}                   | 39.06 | 243.49 | 8  | 7.9756  | 287   | 3.3           | -50.9 | 165.0 | 200 |                     |
| N 6 {34}                   | 39.38 | 244.05 | 10 | 9.9932  | 1,329 | 1.3           | 66.4  | 49.8  | 200 |                     |
| N 7 {36}                   | 39.38 | 244.02 | 5  | 4.9960  | 1,005 | 2.4           | 44.0  | 328.8 | 400 |                     |

TABLE 2 (continued)

|                                       |         |        |    |         |       |     |       |       |     |                              |  |
|---------------------------------------|---------|--------|----|---------|-------|-----|-------|-------|-----|------------------------------|--|
| N 8 (40)                              | 38.85   | 444.73 | 8  | 7.9812  | 372   | 2.9 | -38.3 | 162.3 | 100 | } Needles Range<br>Formation |  |
| N 9 (39)                              | 38.60   | 244.73 | 10 | 9.9689  | 290   | 2.6 | -11.0 | 163.2 | 200 |                              |  |
| N 10 (44)                             | 38.54   | 245.07 | 10 | 9.9518  | 187   | 3.6 | 25.2  | 309.8 | 200 |                              |  |
| N 11                                  | 38.62   | 246.15 | 10 | 5.1698  | ..    | ..  | ..    | ..    | 400 |                              |  |
| N 12 (49)                             | 38.61   | 246.16 | 10 | 9.8912  | 83    | 5.3 | -39.7 | 183.0 | 200 |                              |  |
| N 13 (50)                             | 38.47   | 246.53 | 10 | 9.9786  | 421   | 2.4 | 46.4  | 329.5 | 400 |                              |  |
| } Windous Butte Formation             |         |        |    |         |       |     |       |       |     |                              |  |
| W 1                                   | 38.79   | 243.76 | 10 | 9.99306 | 1,297 | 1.3 | -62.9 | 118.5 | 100 |                              |  |
| W 2                                   | 38.99   | 243.72 | 10 | 9.9906  | 960   | 1.6 | -66.6 | 74.4  | 200 |                              |  |
| W 3                                   | 39.03   | 244.16 | 10 | 9.9522  | 188   | 3.5 | -62.5 | 116.9 | 400 |                              |  |
| W 4                                   | 39.02   | 244.17 | 10 | 9.9886  | 788   | 1.7 | -62.5 | 105.6 | 100 |                              |  |
| W 5                                   | 38.67   | 244.65 | 10 | 9.8680  | 68    | 5.9 | -69.8 | 114.3 | 400 |                              |  |
| W 6                                   | } 38.61 | 244.73 | 12 | 11.8952 | 105   | 4.3 | -60.8 | 127.7 | 400 |                              |  |
| W 7                                   |         |        |    |         |       |     |       |       |     |                              |  |
| W 8 (42)                              | } 38.93 | 244.83 | 10 | 9.9943  | 1,579 | 1.2 | -63.0 | 126.9 | 200 |                              |  |
| W 9                                   |         |        |    |         |       |     |       |       |     |                              |  |
| W 10                                  | } 38.54 | 245.06 | 7  | 6.9957  | 1,396 | 1.6 | -57.2 | 73.8  | 200 |                              |  |
| W 11                                  |         |        |    |         |       |     |       |       |     |                              |  |
|                                       |         |        | 9  | 8.9829  | 467   | 2.4 | -64.4 | 65.2  | 200 |                              |  |
| } Tuff of Pancake Summit              |         |        |    |         |       |     |       |       |     |                              |  |
| P 1                                   | 39.18   | 243.25 | 10 | 9.7271  | 33    | 8.5 | -44.3 | 150.3 | 200 |                              |  |
| P 2                                   | 39.04   | 243.68 | 10 | 9.9231  | 117   | 4.5 | -41.7 | 151.9 | 200 |                              |  |
| P 3                                   | 39.03   | 244.16 | 10 | 9.9921  | 1,134 | 1.4 | -37.2 | 156.4 | 100 |                              |  |
| P 4                                   | 39.21   | 244.25 | 10 | 9.9240  | 118   | 4.5 | -39.7 | 164.0 | 200 |                              |  |
| P 5 (37)                              | 39.40   | 244.28 | 8  | 7.9197  | 87    | 6.0 | -44.1 | 153.9 | 200 |                              |  |
| } Stone Cabin Formation, Upper Member |         |        |    |         |       |     |       |       |     |                              |  |
| S 1                                   | 39.21   | 244.25 | 9  | 8.9847  | 522   | 2.3 | 27.8  | 27.9  | 200 |                              |  |
| S 2                                   | 39.03   | 244.14 | 10 | 9.9462  | 167   | 3.8 | 30.6  | 46.6  | 200 |                              |  |
| S 3 (38)                              | 38.67   | 244.65 | 12 | 11.9589 | 268   | 2.7 | 22.2  | 44.6  | 200 |                              |  |
| S 4                                   | 38.61   | 244.73 | 11 | 10.9768 | 431   | 2.2 | 19.4  | 27.9  | 200 |                              |  |

Lat., Long., north latitude and east longitude of site, degrees; N, number of specimens; R, vector resultant length of *N* unit vectors; *k*, precision parameter (Fisher, 1953); *Os*, sample of cone of 95 percent confidence of mean, degrees; *I*, *D*, inclination (positive downward) and declination (east of north) of mean *VRN* direction, degrees; *H*, peak alternating field in which specimens were demagnetized, oersteds.

\*Site numbers in brackets are those of Cromie and McKee (in preparation).

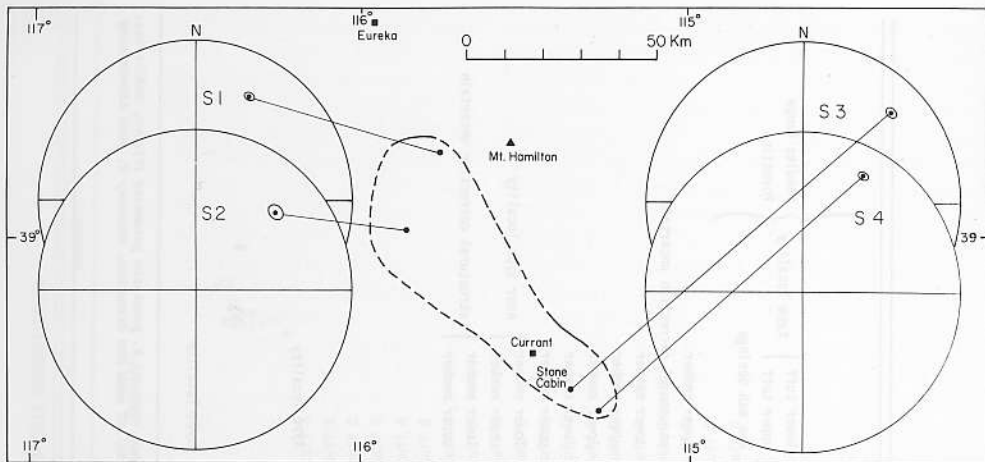


Figure 3. NRM directions, sampling localities, and geographic extent: upper cooling unit of the Stone Cabin Formation. NRM directions (dots) are plotted on lower hemisphere of equal-area projections with as-

sociated 95 percent confidence circles (Table 1). Margin of ash-flow sheet is dashed where approximate or inferred, solid where mapped in the field.

ash-flow sheets are distinctly different. This was the first indication that there are two different ash-flow cooling units; later investigation revealed the two similar cooling units occurring together in the expected stratigraphic relation at sites P3, W3, and W4 near Big Louis Spring.

The lateral extent of the Windous Butte Formation determined by us (Fig. 5) is considerably less than was shown by Cook (1965). Part of this difference is due to the recognition of the tuff of Pancake Summit, which has made it possible to draw the northern margin of the Windous Butte Formation approximately 50 km farther south than shown by Cook. Additional mapping has outlined the northeastern and western limits of the ash-flow sheet as well as the northern boundary, but the southern and southeastern boundaries are much less certain. We have omitted an

area to the southeast in which Cook stated that the lower member was absent and the upper member was only possibly present, and have arbitrarily moved the southern margin 40 to 60 km northward. The Windous Butte Formation is not present in the vicinity of Morey Peak, nor is it present in the southern Pancake Range section about 50 km southeast of Morey Peak, where Cook had tentatively shown a thickness of 250 m (W. D. Quinlivan and W. J. Carr, 1969, oral commun.). It may, however, extend farther south of the vicinity of Sunnyside than shown in Figure 5. The maximum linear extent is about 150 km in an east-west direction from the Hot Creek Range to the Egan Range (Fig. 1), and the area as shown in Figure 5 is about 8,200 km<sup>2</sup>. Using Cook's (1965) average thickness of 160 m gives a minimum of about 1,300 km<sup>3</sup> for the combined volume of both Windous Butte cooling units,

TABLE 3. DECREASE OF ANGULAR DISPERSION BETWEEN SITE-MEAN NRM DIRECTIONS IN SINGLE ASH-FLOW SHEETS AFTER STRUCTURAL CORRECTION

| Formation                   | N  | $k_1$ | $k_2$ | r    | $\alpha_{95}$ | Significant at 95 percent(?) |
|-----------------------------|----|-------|-------|------|---------------|------------------------------|
| Tuff of Clipper Gap         | 6  | 37    | 107   | 2.89 | 2.97          | no                           |
| Bates Mountain Tuff, unit D | 7  | 32    | 121   | 3.78 | 2.69          | yes                          |
| Windous Butte Formation     | 11 | 53    | 60    | 1.13 | 2.12          | no                           |
|                             | 8* | 53    | 266   | 5.02 | 2.48          | yes                          |
| Tuff of Pancake Summit      | 5  | 42    | 259   | 6.17 | 3.44          | yes                          |
| Stone Cabin                 | 4  | 23    | 59    | 2.57 | 4.28          | no                           |

N, number of sites;  $k_1$ , precision parameter before structural correction;  $k_2$ , precision parameter after structural correction; r, ratio  $k_1/k_2$ ;  $\alpha_{95}$ , 95 percent significance level of r for specified N (McElhinney, 1964).

\*Sites W2, W10, W11 omitted.

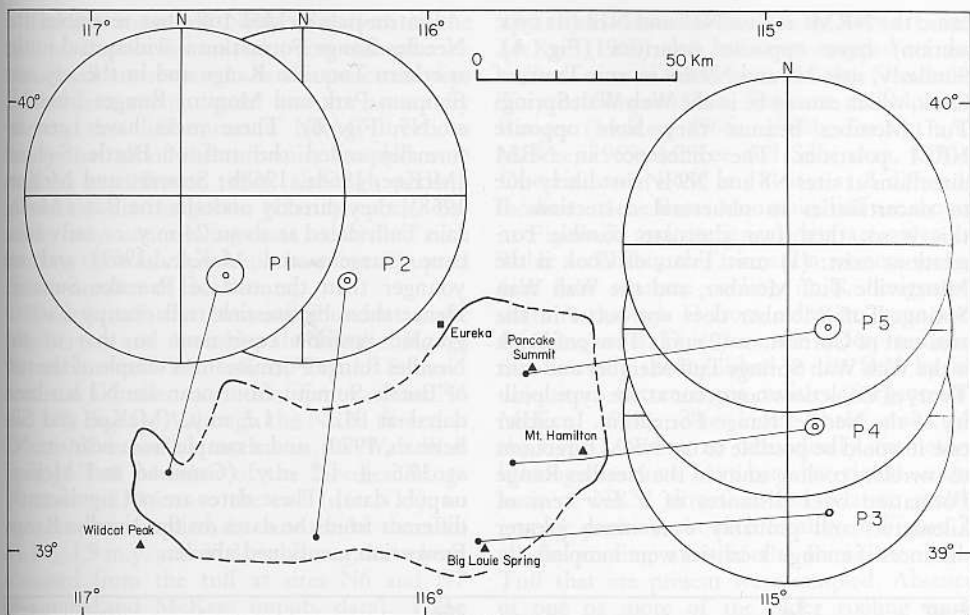


Figure 4. NRM directions, sampling localities, and distribution of the tuff of Pancake Summit. NRM directions (open circles) are plotted on upper hemi-

sphere of equal-area projections; other conventions as in Figure 3.

somewhat less than Cook's estimate of 1,800 km<sup>2</sup>.

#### Needles Range Formation and Other Biotite-Rich Tuffs

By far the most extensive Tertiary ash-flow sheet in the Great Basin is the Needles Range Formation. These distinctive biotite-rich welded tuffs were considered by Mackin (1960) and Cook (1965) to extend from the Paunsaugunt Plateau in Utah westward at least to the Grant Range, Nevada, a distance of more than 300 km, and to cover an area of some 34,000 km<sup>2</sup>. As first described and named by Mackin (1960), this formation consisted of two to three ash-flow sheets occurring in the Needles Range of southwestern Utah. The lower member was named the Wah Wah Springs Tuff after its occurrence just south of Wah Wah Springs 30 km east of the type Needles Range. The upper member in the Needles Range was named the Minersville Tuff for its occurrence in Minersville Canyon. Cook described five members of the Needles Range Formation in eastern Nevada, the lower two of which he thought correlated with the Wah Wah Springs and Minersville Tuff Members in Utah. Consistent K-Ar ages have been determined

on samples from the Needles Range Formation; Kistler (1968) obtained dates of 29.3 and 29.2 m.y. on biotite and hornblende, respectively, from a locality in Utah, and Armstrong (1970) obtained 14 dates from 12 localities in Utah and Nevada that averaged  $29.7 \pm 0.3$  m.y.

Six localities in the Needles Range Formation were sampled for this study. The magnetic data are given in Table 2, and the NRM directions and sampling localities are shown in Figure 6. Site N11 is the only locality for which the effects of remagnetization by lightning could not be removed by a.f. demagnetization. The NRM direction for this site shown in Figure 6 is an estimate of the locus of intersection of the great-circle paths followed by the individual NRM directions during demagnetization. The direction shown for site N11, which is in the Wah Wah Springs Tuff Member at the Needles Range type locality, is nearly identical to that for site N13, which is in the same cooling unit at Wah Wah Springs. Site N12 is in the Minersville Tuff Member at the Needles Range Type locality; this cooling unit was not sampled anywhere to the east.

Site N10 is in unit T<sub>Vnr</sub><sub>2</sub> of Cook (1965) at Shingle Spring in the Egan Range; clearly this cannot be in the Minersville Tuff Member be-

cause the NRMs at sites N10 and N12 (its type section) have opposite polarities (Fig. 6). Similarly, sites N8 and N9 are in unit  $T_{vnr1}$  of Cook, which cannot be in the Wah Wah Springs Tuff Member because they have opposite NRM polarities. The difference in NRM directions at sites N8 and N9 is most likely due to uncertainties in structural correction. If this is so, then two alternate possible correlations exist: (1) unit  $T_{vnr1}$  of Cook is the Minersville Tuff Member, and the Wah Wah Springs Tuff Member does not occur in the area east of Currant, or (2) unit  $T_{vnr2}$  of Cook is the Wah Wah Springs Tuff Member and unit  $T_{vnr1}$  of Cook does not occur at the type locality of the Needles Range Formation. In either case it would be possible to use NRM directions to correlate cooling units in the Needles Range Formation over distances of a few tens of kilometers and probably over much greater distances if enough localities were sampled.

Biotite-rich welded tuff that resembles the Needles Range Formation is widespread in the northern Toquima Range and in the adjacent Simpson Park and Monitor Ranges (sites N1 to N5, Fig. 6). These rocks have been informally called the tuff of Bottle Summit (McKee, 1968a, 1968b; Stewart and McKee, 1968); they directly underlie the Bates Mountain Tuff, dated at about 24 m.y. or early Miocene (Sargent and McKee, 1969) and are younger than the tuff of Pancake Summit. Hence these biotite-rich tuffs occupy a stratigraphic position equivalent to that of the Needles Range Formation. A sample of the tuff of Bottle Summit from near site N3 has been dated at  $31.1 \pm 1.2$  m.y. (McKee and Silberman, 1970), and a sample from near site N2 at  $30.6 \pm 1.2$  m.y. (Grommé and McKee, unpub. data). These dates are not significantly different from the dates on the Needles Range Formation mentioned above.

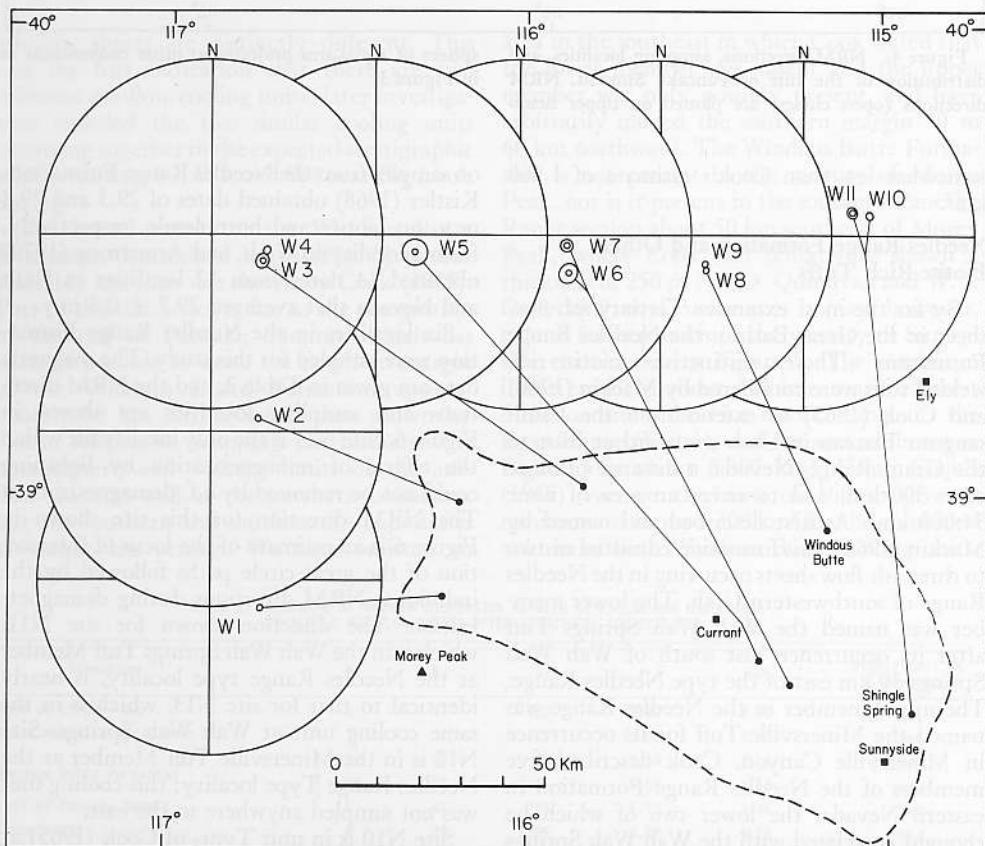


Figure 5. NRM directions, sampling localities, and approximate distribution of both cooling units of the Windous Butte Formation. Conventions as in Figures 2 and 3.

The five measured NRM directions in the tuff of Bottle Summit do not coincide, although all are reversed. As the structural dips in this area are not great and are accurately known, the differences in NRM directions imply that all of the tuff units sampled were erupted at different times, although perhaps all within one magnetic polarity epoch. Because only one cooling unit occurs at each locality, these ash-flows must have been erupted from a number of local vents.

Welded tuff that contains abundant mafic phenocrysts and resembles the Needles Range Formation and the tuff of Bottle Summit occurs in a small area south of Eureka (sites N6 and N7, Fig. 6). Although the NRM direction at site N7 is similar to that in the Wah Wah Springs Tuff Member of the Needles Range Formation 230 km to the east (site N13), no correlation is implied, because K-Ar dates of  $34.3 \pm 1.9$  m.y. and  $35.3 \pm 1.9$  m.y. have been obtained from the tuff at sites N6 and N7 (Grommé and McKee, unpub. data). These dates are significantly older than those from the Needles Range Formation.

#### Bates Mountain Tuff

The Bates Mountain Tuff is a sequence of rhyolitic crystal-poor welded ash-flow cooling units that are widespread in central Nevada.

This formation was named by Stewart and McKee (1968) and has been mapped or described over a wide area in the Shoshone, Toiyabe, Simpson Park, Toquima, and Monitor Ranges (McKee, 1968a, 1968b; Sargent and McKee, 1969; McKee and Silberman, 1970). Directions of NRM at 17 sites at 8 different localities in the Bates Mountain Tuff are shown in Figure 7, and numerical data are given in Table 1. Within this formation we now recognize four separate cooling units, designated units A through D from oldest to youngest. Of these units, D is the most widespread and can be easily distinguished in the field by its ubiquitous flattened gas cavities (Sargent and McKee, 1969). The lower three units, A through C, having no individually distinctive lithologic features, have been correlated on the basis of NRM direction and relative stratigraphic position. At each locality in Figure 7, all the cooling units of the Bates Mountain Tuff that are present were sampled. Absence of one or more of the older cooling units beneath unit D suggests, but does not prove, that they were never present. Sufficient time elapsed between the eruptions of each ash flow for a geomagnetic reversal to occur, but this minimum time is only of the order of 2,000 to 20,000 yrs (Cox and Dalrymple, 1967). There is some indication from the K-Ar dates

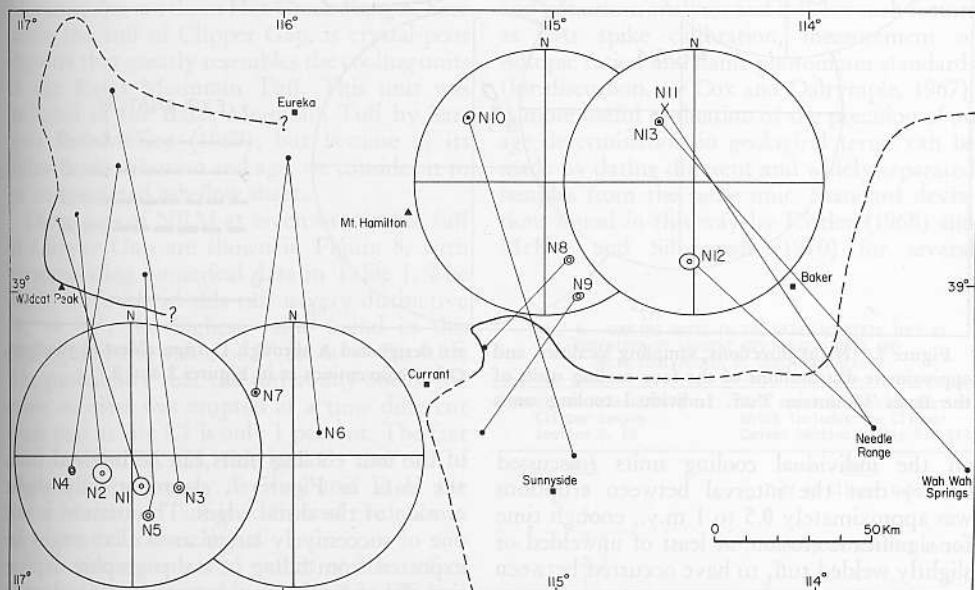


Figure 6. NRM directions and sampling localities in the Needles Range Formation (N8 to N13) and other

biotite-rich tuffs (N1 to N7). Conventions as in Figures 2 and 3.

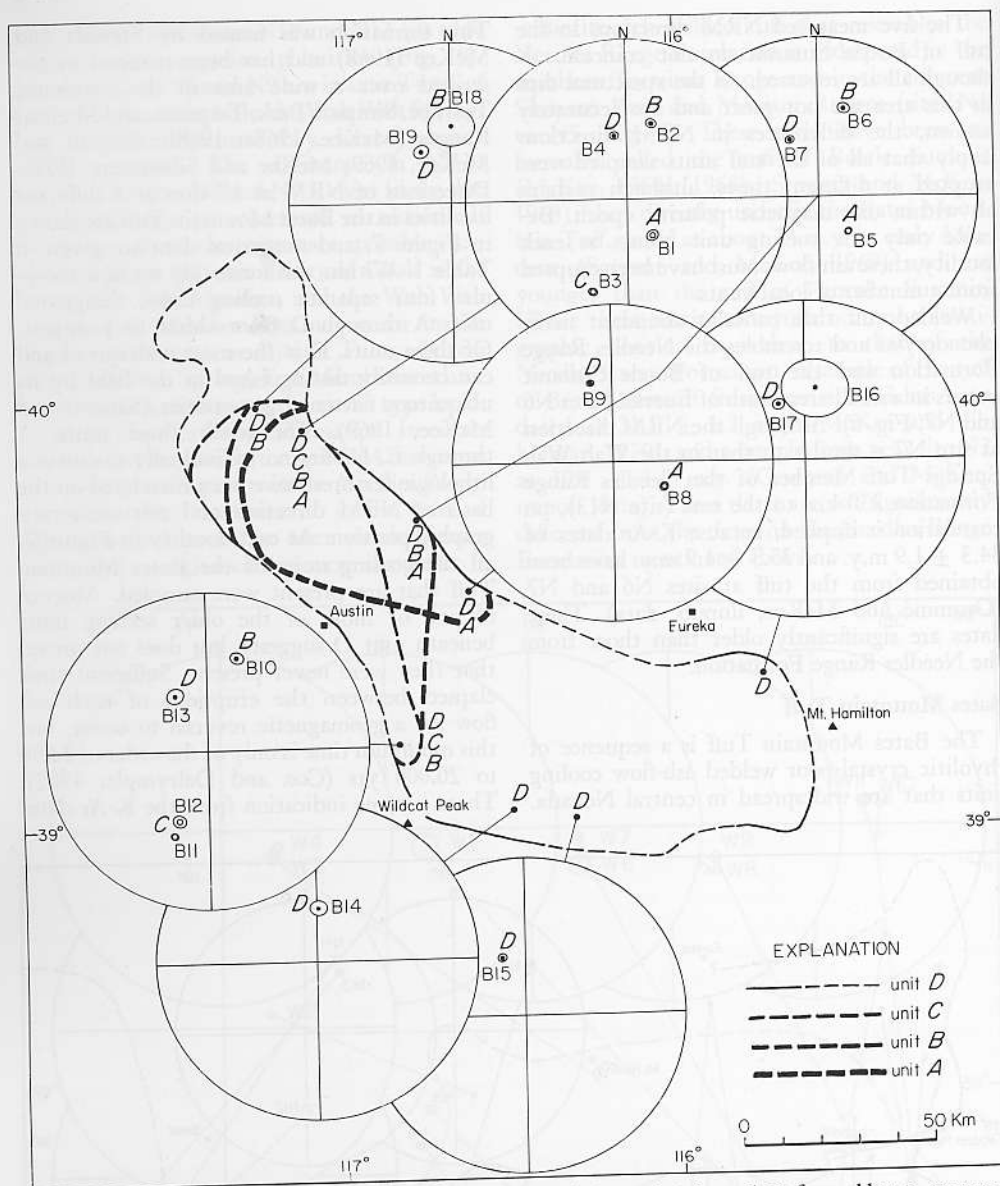


Figure 7. NRM directions, sampling localities, and approximate distributions of the four cooling units of the Bates Mountain Tuff. Individual cooling units

are designated A through D from oldest to youngest. Other conventions as in Figures 2 and 3.

on the individual cooling units (discussed below) that the interval between eruptions was approximately 0.5 to 1 m.y., enough time for significant erosion, at least of unwelded or slightly welded tuff, to have occurred between eruptions.

A distribution pattern of the welded parts

of the four cooling units can be inferred from the data in Figure 7, assuming only slight erosion of the distal edges. The pattern is not one of successively larger areas that might be expected from filling of a topographic depression; for example, unit A occupies a northwest-trending area north of the town of Austin,

whereas unit C apparently occurs in a north-trending area not including the two eastern localities where unit A was found. The four cooling units of the Bates Mountain Tuff may have come from a common source north of Austin in the area between the Shoshone and Toiyabe Ranges, but this is uncertain.

The most detailed description of the stratigraphy of the Bates Mountain Tuff is by Sargent and McKee (1969), who confined their discussion to the southwestern part of the area shown in Figure 7. The nomenclature used by Sargent and McKee has been modified in this paper (Table 4). Unit 5 of Sargent and McKee, which resembles several of the tuff units in the Bates Mountain Tuff, has a different distribution and is significantly younger. For these reasons, it is not included in the Bates Mountain Tuff in this paper.

Of all the cooling units of the Bates Mountain Tuff, unit D is the most extensive, having a maximum linear extent of 220 km and an area of about 8,200 km<sup>2</sup>. The average thickness of this unit is 16 m, giving it a volume of about 160 km<sup>3</sup>. Areas and thickness of the older cooling units (A, B, and C) are less well known, but the total volume of all units in the Bates Mountain Tuff may be as great as 500 km<sup>3</sup>.

#### Tuff of Clipper Gap

The youngest ash-flow sheet in the Toquima, Monitor, and northern Hot Creek Ranges, here called the tuff of Clipper Gap, is crystal-poor rhyolite that greatly resembles the cooling units of the Bates Mountain Tuff. This unit was included in the Bates Mountain Tuff by Sargent and McKee (1969), but because of its different distribution and age, we consider it to be an unrelated ash-flow sheet.

Directions of NRM at seven sites in the tuff of Clipper Gap are shown in Figure 8, with corresponding numerical data in Table 1. The NRM direction in this tuff is very distinctive ( $\delta_a = 64^\circ$ , the highest value found in this study), and the value of  $P'$  for  $n = 7$  is 0.01. The probability that the tuff at any one of the other six sites was erupted at a time different from that at site C1 is only 1 percent. The fact that at sites C1, C2, C3, and C4 the tuff of Clipper Gap directly overlies unit D of the Bates Mountain Tuff is additional evidence in support of this correlation.

The maximum lateral extent of the tuff of Clipper Gap as shown in Figure 8 is 185 km. Like the other ash-flow sheets, the original

extent must have been somewhat greater. The area shown in Figure 8 is approximately 6,300 km<sup>2</sup>, and taking the average thickness as 30 m, the minimum volume of the tuff of Clipper Gap is approximately 190 km<sup>3</sup>.

#### K-AR AGES

Potassium-argon age determinations were made for some of the ash-flow sheets discussed in the preceding section. All analyses were made on either biotite or sanidine separated from the rocks, and standard analytical methods were employed (Dalrymple and Lanphere, 1969). Argon was measured by the isotope-dilution method, and potassium was determined by flame photometer. The decay constants used for <sup>40</sup>K were  $\lambda_e = 0.585 \times 10^{-10}$  yr<sup>-1</sup> and  $\lambda_\beta = 4.72 \times 10^{-10}$  yr<sup>-1</sup>, and the atomic abundance of <sup>40</sup>K/ $K_{total}$  is  $1.19 \times 10^{-4}$  atom/atom. These age determinations supplement in part those published by Armstrong (1970) mentioned above; our results are in good agreement.

The analytical data and calculated ages are given in Table 5. The uncertainties given in Table 5 for the individual ages range from 2 percent to 2.5 percent and are assigned on the basis of a statistical evaluation of a number of replicate argon and potassium analyses (McKee and Silberman, 1970). These values represent only the cumulative uncertainties in argon and potassium analyses and involve such factors as <sup>38</sup>Ar spike calibration, measurement of isotopic ratios, and flame photometer standards (for discussion, see Cox and Dalrymple, 1967). A more useful evaluation of the precision of an age determination in geological terms can be made by dating different and widely separated samples from the same unit. Standard deviations found in this way by Kistler (1968) and McKee and Silberman (1970) for several

TABLE 4. COOLING UNITS IN THE BATES MOUNTAIN TUFF AS DESCRIBED BY SARGENT AND MCKEE (1969) AND THEIR EQUIVALENTS AS DESCRIBED HEREIN

| Sargent and McKee (1969)<br>Clipper Canyon<br>Section p. E6 | This paper (composite section<br>which includes the Clipper<br>Canyon Section, sites B10-B13) |
|---|---|
| Unit  | Unit  |
| 5   | Tuff of Clipper Gap   |
| 4   | D   |
| 3   | C (Compound cooling unit)   |
| 2   |   |
| 1   | B   |
|   | A   |

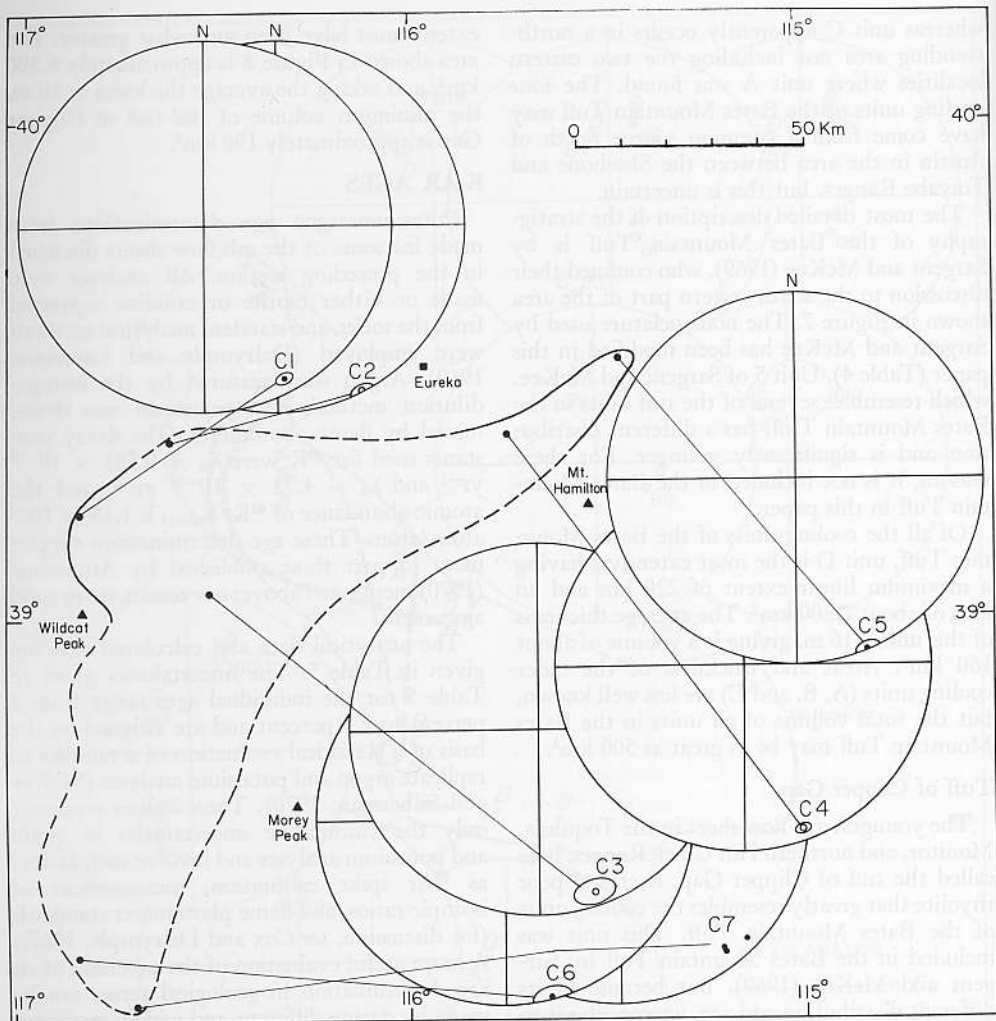


Figure 8. NRM directions, sampling localities, and distribution of the tuff of Clipper Gap. Conventions as

in Figures 2 and 3. Data for site C7 are from Sargent and McKee (1969).

Tertiary ash-flow sheets are between 3 percent and 4 percent.

The age data in this study are well suited for evaluation of K-Ar ages of widespread volcanic units, because the paleomagnetic data assure correct correlation of cooling units, minimizing the possibility of real differences in ages of samples thought to be from the same cooling unit. In each of the older crystal-rich ash-flow units, samples were dated from several localities separated as widely as possible and, in most cases, both biotite and sanidine from the sample were analyzed. The variations of the calculated ages include such factors as possible differences

in argon retentivity in sanidine or biotite in different parts of the tuff sheets, or possible local post-eruption reheating. The mean ages and their standard deviations for three crystal-rich tuffs are given in Table 6. Standard deviations range from 2.1 percent to 4.2 percent, and the pooled estimate (McIntyre, 1963) for the three ash-flow sheets is 3.0 percent with upper and lower 95 percent confidence limits of 4.4 percent and 2.2 percent (Crow and others, 1960). This value is the same as that found by McKee and Silberman (1970), who used fewer samples but a wider variety of rock types.

Inspection of the calculated ages for paired

TABLE 5. K-Ar AGES, WITH ANALYTICAL DATA

| Site no.                                  | Mineral analyzed | wt. percent    | $^{40}\text{Ar}$ rad<br>moles/gm $\times 10^{-10}$ | $^{40}\text{Ar}$ rad $\times 100$<br>$^{40}\text{Ar}$ total | Age, $10^6$ years | Remarks                           |
|---|------------------|----------------|--|---|-------------------|-----------------------------------|
| <u>Tuff of Clipper Gap</u>                |                  |                |  |   |                   |                                   |
| C 4                                       | sanidine         | 8.02           | 3.60   | 82.0  | 22.1 $\pm$ 0.6    |                                   |
| <u>Bates Mountain Formation, Tuff D</u>   |                  |                |  |   |                   |                                   |
| B 17                                      | sanidine         | 10.80<br>10.88 | 3.71   | 82.4  | 23.1 $\pm$ 0.6    |                                   |
| <u>Windous Butte Formation</u>            |                  |                |  |   |                   |                                   |
| W 1                                       | sanidine         | 12.35<br>12.37 | 5.70   | 62.1  | 30.9 $\pm$ 0.8    | lower member                      |
| W 3                                       | sanidine         | 12.82<br>12.88 | 5.80   | 82.9  | 30.3 $\pm$ 0.8    | lower member                      |
|   | biotite          | 8.78<br>8.78   | 4.14   | 49.1  | 31.7 $\pm$ 0.8    |                                   |
| W 4                                       | sanidine         | 13.03<br>13.05 | 5.79   | 83.6  | 29.8 $\pm$ 0.8    | upper member                      |
|   | biotite          | 8.73<br>8.74   | 4.12   | 39.8  | 31.6 $\pm$ 0.8    |                                   |
| W 8                                       | sanidine         | 13.05<br>13.12 | 5.88   | 68.9  | 30.2 $\pm$ 0.8    | lower member                      |
|   | biotite          | 8.83<br>8.87   | 4.04   | 80.6  | 30.7 $\pm$ 0.8    |                                   |
| W 9                                       | sanidine         | 12.34<br>12.35 | 5.59   | 73.0  | 30.3 $\pm$ 0.8    | upper member                      |
|   | biotite          | 8.35<br>8.37   | 3.82   | 77.0  | 30.7 $\pm$ 0.8    |                                   |
| <u>Tuff of Pancake Summit</u>             |                  |                |  |   |                   |                                   |
| P 1                                       | sanidine         | 12.08<br>12.10 | 5.63   | 90.6  | 31.3 $\pm$ 0.8    |                                   |
| P 2                                       | sanidine         | 12.03<br>12.05 | 5.40   | 77.5  | 30.1 $\pm$ 0.8    |                                   |
|   | biotite          | 8.36<br>8.39   | 3.83   | 41.0  | 30.7 $\pm$ 0.8    |                                   |
| P 3                                       | sanidine         | 12.39<br>12.43 | 6.02   | 89.1  | 32.5 $\pm$ 0.8    | Big Louie Spring                  |
|   | biotite          | 8.75<br>8.75   | 4.42   | 67.8  | 33.9 $\pm$ 0.9    |                                   |
| P 4                                       | biotite          | 8.30<br>8.66   | 4.04   | 82.0  | 32.6 $\pm$ 0.8    |                                   |
|   | biotite          | 8.68<br>8.72   | 4.23   | 74.5  | 32.9 $\pm$ 0.8    |                                   |
| <u>Stone Cabin Formation Upper Member</u> |                  |                |  |   |                   |                                   |
| S 2                                       | sanidine         | 12.58<br>12.59 | 6.22   | 86.3  | 33.2 $\pm$ 0.8    | Big Louie Spring                  |
|   | biotite          | 7.73<br>7.80   | 4.04   | 48.3  | 34.8 $\pm$ 0.9    |                                   |
| S 3                                       | sanidine         | 12.84<br>13.00 | 6.46   | 90.0  | 33.4 $\pm$ 0.8    | Stone Cabin<br>(at type locality) |
|   | biotite          | 13.07<br>8.25  | 4.30   | 41.5  | 34.9 $\pm$ 0.9    |                                   |
|   | biotite          | 8.25           |  |   |                   |                                   |

sanidine and biotite from the same sites suggests that consistently lower values are obtained from sanidine. The average difference is 3.3 percent and is statistically significant at the 95 percent level of confidence; it contributes

appreciably to the pooled standard deviation of 3.0 percent. The reason for the younger apparent sanidine ages is not known with certainty, although Webb and McDougall (1967), who observed a similar effect, suggested

TABLE 6. MEAN K-Ar AGES AND STANDARD DEVIATIONS FROM BIOTITE AND SANIDINE SEPARATED FROM CRYSTAL-RICH ASH-FLOW SHEETS FROM DATA IN TABLE 5

|                                    | Mean age            | S.D.                | S.D. | N  |
|------------------------------------|---------------------|---------------------|------|----|
|                                    | 10 <sup>6</sup> yrs | 10 <sup>6</sup> yrs | %    |    |
| Windous Butte Formation            | 30.7                | 0.6                 | 2.1  | 9  |
| Tuff of Pancake Summit             | 32.0                | 1.3                 | 4.2  | 7  |
| Stone Cabin Formation upper member | 34.1                | 0.9                 | 2.6  | 4  |
| Pooled estimate                    | ..                  | ..                  | 3.0  | 20 |

that it may be due to incomplete removal of argon from sanidine during fusion in the gas-extraction procedure. Our preliminary experiments using various fusion temperatures and times have not confirmed this, and there is not yet sufficient evidence to conclude that the biotite ages are more or less reliable than the sanidine ages.

In addition to those given in Table 5, K-Ar ages from the Bates Mountain Tuff and the tuff of Clipper Gap have been published in other papers. All ages determined from these rocks are summarized in Table 7. Note that there are no stratigraphic discordances; this suggests that the relative precision of this group of age determinations may be better than 3 percent. The average rate of eruption of these crystal-poor ash-flows is on the order of one every 0.8 m.y., which does not conflict with the fact that a geomagnetic reversal occurred between each eruption.

## SUMMARY AND CONCLUSIONS

The widespread ash-flow sheets that make up most of the Tertiary rocks in the central Great Basin have been extensively correlated on the basis of lithology and stratigraphic position. The purpose of this work has been to test these correlations by comparison of directions of natural remanent magnetization (NRM) in the individual ash-flow cooling units. The principle of this method rests on the fact that because the average frequency of eruption of ash flows is much less than the characteristic rate of secular variation of the direction of the geomagnetic field, the directions of thermoremanent mag-

netization in successive cooling units are significantly different. In a given volcanic province, the NRM direction is a unique characteristic of each ash-flow cooling unit.

The six ash-flow sheets investigated here were chosen because their distribution was fairly well known; they have not undergone severe alteration or tectonic deformation (faulting or folding); and they are representative of the lithologic types erupted over a period of several million years. They comprise, from oldest to youngest, the Stone Cabin Formation, the tuff of Pancake Summit, the Windous Butte Formation, the Needles Range Formation, the Bates Mountain Tuff, and the tuff of Clipper Gap. Potassium-argon ages of these ash-flow sheets range from 34 to 22 m.y. (Oligocene to early Miocene). The minimum time interval between eruptions of individual but related cooling units is roughly 0.8 m.y.

The paleomagnetic data have confirmed most of the lithologic correlations, and have allowed more accurate delineation of individual cooling units than was previously possible. In particular, the distinction between the Windous Butte Formation and the tuff of Pancake Summit, and the separation of the tuff of Clipper Gap from the Bates Mountain Tuff are based on their NRM directions. The enormous volumes of eruptive material represented by some of the cooling units in these ash-flow sheets and their broad distributions are summarized in Table 1. Because ash-flow tuff makes up much of the Tertiary stratigraphic section, it is the key to a large part of the Tertiary history of the central part of the Great Basin. The distances over which these paleomagnetic correlations have been made range up to 200 km; thus they are particularly useful in the Basin and Range province where outcrops are confined to mountain ranges separated by alluvium-filled valleys.

## ACKNOWLEDGMENTS

We thank Richard K. Hose, John H. Stewart, William D. Quinlivan, and Will H.

TABLE 7. POTASSIUM-ARGON AGES DETERMINED FROM SANIDINES IN CRYSTAL-POOR ASH-FLOW SHEETS

|                      |                |                |                |
|----------------------|----------------|----------------|----------------|
| Tuff of Clipper Gap  | 22.1 ± 0.7 (a) | 22.2 ± 0.7 (b) |                |
| Bates Mountain Tuff: |                |                |                |
| Unit D               | 23.1 ± 0.7 (a) | 22.8 ± 0.7 (b) | 23.3 ± 0.7 (c) |
| Unit B or C*         | 24.1 ± 0.7 (d) | 23.9 ± 0.7 (c) | 23.7 ± 0.7 (b) |
| Unit A               | 24.7 ± 0.7 (d) |                |                |

References: (a) this paper; (b) Sargent and McKee, 1969; (c) McKee and Stewart, 1971; (d) McKee and Silberman, 1970.  
\*These cooling units were not separately identified when samples were collected.

Carr for helpful discussions in the field. Richard V. Clark, James E. Leonard, and Edward A. Mankinen assisted in the field and made the magnetic measurements. F. M. Byers, Jr., kindly provided petrographic modal analyses of some of the crystal-rich ash-flow sheets. The age of 32.6 m.y. for the tuff of Pancake Summit at site P4 was determined by Richard F. Marvin. The geologic mapping was done in conjunction with the Nevada Bureau of Mines county map program.

#### APPENDIX. STATISTICAL ANALYSIS OF PAIRED MINERAL ANALYSES

The significance of the apparent systematic differences between ages determined for sanidine and biotite from the same hand specimens was evaluated as follows:

$N$  = number of biotite sanidine pairs  
= 9

$M$  = overall mean of paired ages =  
31.91 m.y.

$a_s, a_b$  = individual calculated ages of  
sanidine and biotite,  
respectively, from Table 5

$A_s, A_b$  = normalized ages of sanidine and  
biotite, where:

$$A_{s,b} = a_{s,b} \frac{2M}{a_s + a_b}$$

The average normalized ages are:

|         | sanidine    | biotite     |
|---------|-------------|-------------|
| average | 31.38 m.y.  | 32.43 m.y.  |
| S.D.    | $\pm 0.289$ | $\pm 0.290$ |

The difference between the normalized ages is 1.05 m.y., or 3.3 percent of the overall mean. The critical value at a probability level of 0.1 is (McIntyre, 1963):

$$C.V. = 3.643 \frac{S.D.}{\sqrt{N}} = 0.35 = 1.1 \text{ percent.}$$

Hence there is a greater than 99 percent probability that the calculated sanidine ages are significantly lower than the calculated biotite ages.

#### REFERENCES CITED

- Armstrong, R. L., 1970, Geochronology of Tertiary igneous rocks, eastern Basin and Range province, western Utah, eastern Nevada, and vicinity, U.S.A.: *Geochim. et Cosmochim. Acta*, v. 34, p. 203-232.
- Cook, E. F., 1965, Stratigraphy of Tertiary volcanic rocks in eastern Nevada: Nevada Bur. Mines Rept. 11.
- Cox, A., 1961, Anomalous remanent magnetization of basalt: U.S. Geol. Survey Bull. 1083-E, p. 131-160.
- 1971, Remanent magnetization and susceptibility of late Cenozoic rocks from New Zealand: *New Zealand Jour. Geology and Geophysics*, v. 14, p. 192-207.
- Cox, A., and Dalrymple, G. B., 1967, Statistical analysis of geomagnetic reversal data and the precision of potassium-argon dating: *Jour. Geophys. Research*, v. 72, p. 2603-2614.
- Crow, E. L., Davis, F. A., and Maxfield, M. W., 1960, *Statistics manual*. New York, Dover Publications, Inc., 288 p.
- Dalrymple, G. B., and Lanphere, M. A., 1969, Potassium-argon dating. Principles, techniques, and applications to geochronology: San Francisco, W. H. Freeman and Co., 258 p.
- Dalrymple, G. B., Cox, A., and Doell, R. R., 1965, Potassium-argon age and paleomagnetism of the Bishop Tuff, California: *Geol. Soc. America Bull.*, v. 76, p. 665-673.
- Doell, R. R., 1970, Paleomagnetic secular variation study of lavas from the Massif Central, France: *Earth and Planetary Sci. Letters*, v. 8, p. 352-362.
- Doell, R. R., and Cox, A., 1965, Measurement of the remanent magnetization of igneous rocks: U.S. Geol. Survey Bull. 1203-A, p. A1-A32.
- 1967a, Paleomagnetic sampling with a portable coring drill, in Collinson, D. W., Creer, K. M., and Runcorn, S. K., eds., *Developments in solid earth geophysics 3: Methods in paleomagnetism*: Amsterdam, Elsevier Publishing Co., p. 21-25.
- 1967b, Analysis of spinner magnetometer operation, in Collinson, D. W., Creer, K. M., and Runcorn, S. K., eds., *Developments in solid earth geophysics 3: Methods in paleomagnetism*: Amsterdam, Elsevier Publishing Co., p. 196-206.
- 1967c, Analysis of alternating field demagnetization equipment, in Collinson, D. W., Creer, K. M., and Runcorn, S. K., eds., *Developments in solid earth geophysics 3: Methods in paleomagnetism*: Amsterdam, Elsevier Publishing Co., p. 241-253.
- Fisher, R. A., 1953, Dispersion on a sphere: *Royal Soc. [London] Proc.*, ser. A, v. 217, p. 295-305.
- Fuller, M. D., 1963, Magnetic anisotropy and paleomagnetism: *Jour. Geophys. Research*, v. 68, p. 293-309.
- Gilbert, C. M., 1938, Welded tuff in eastern California: *Geol. Soc. America Bull.*, v. 49, p. 1829-1862.
- Gose, W. A., 1970, Paleomagnetic studies of Miocene ignimbrites from Nevada: *Royal Astron. Soc. Geophys. Jour.*, v. 20, p. 241-252.
- Graham, K.W.T., 1961, The re-magnetization of a

- surface outcrop by lightning currents: *Royal Astron. Soc. Geophys. Jour.*, v. 6, p. 85-102.
- Grommé, C. S., and McKee, E. H., 1971, Mid-Tertiary paleomagnetic pole from volcanic rocks in the western United States [abs.]: *Am. Geophys. Union Trans.*, v. 52, p. 187.
- Grommé, C. S., Reilly, T. A., Mussett, A. E., and Hay, R. L., 1971, Paleomagnetism and potassium-argon ages of Pleistocene volcanic rocks from Ngorongoro caldera, Tanzania: *Royal Astron. Soc. Geophys. Jour.*, v. 22, p. 101-115.
- Hatherton, T., 1954, The magnetic properties of the Whakamaru Ignimbrites: *New Zealand Jour. Sci. Technology*, ser. B, v. 35, p. 421-432.
- Hose, R. K., and Blake, M. C., Jr., 1970, Geologic map of White Pine County, Nevada: U.S. Geol. Survey open file map.
- Kellogg, H. E., 1964, Cenozoic stratigraphy and structure of the southern Egan Range, Nevada: *Geol. Soc. America Bull.*, v. 75, p. 949-968.
- Kistler, R. W., 1968, Potassium-argon ages of volcanic rocks in Nye and Esmeralda Counties, Nevada: *Geol. Soc. America Mem.* 110, p. 251-262.
- Mackin, J. H., 1960, Structural significance of Tertiary volcanic rocks in southwestern Utah: *Am. Jour. Sci.*, v. 258, p. 81-131.
- McElhinny, M. W., 1964, Statistical significance of the fold test in paleomagnetism: *Royal Astron. Soc. Geophys. Jour.*, v. 8, p. 338-340.
- McIntyre, D. G., 1963, Precision and resolution in geochronometry, in Albritton, C. C., ed., *The fabric of geology*: Stanford, Freeman and Cooper, 374 p.
- McKee, E. H., 1968a, Geologic map of the Ackerman Canyon quadrangle, Nevada: U.S. Geol. Survey Geol. Quad. Map GQ-761.
- 1968b, Geologic map of the Spencer Hot Springs quadrangle, Nevada: U.S. Geol. Survey Geol. Quad. Map GQ-770.
- McKee, E. H., and Silberman, M. L., 1970, Geochronology of Tertiary igneous rocks in central Nevada: *Geol. Soc. America Bull.*, v. 81, p. 2317-2328.
- McKee, E. H., and Stewart, J. H., 1971, Stratigraphy and potassium-argon ages of some Tertiary tuffs in Lander and Churchill Counties, central Nevada: U.S. Geol. Survey Bull. 1311-B, p. B1-B28.
- Nagata, T., 1961, *Rock magnetism*: Tokyo, Maruzen, 350 p.
- Noble, D. C., Bath, G. D., Christiansen, R. L., and Orkild, P. P., 1968, Zonal relations and paleomagnetism of the Spearhead and Rocket Wash members of the Thirsty Canyon Tuff, southern Nevada, in *Geological Survey Research 1968*: U.S. Geol. Survey Prof. Paper 600-C, p. C61-C65.
- Ross, C. S., and Smith, R. L., 1961, Ash-flow tuffs—Their origin, geologic relations, and identification: U.S. Geol. Survey Prof. Paper 366, 81 p.
- Sargent, K. A., and McKee, E. H., 1969, The Bates Mountain Tuff in northern Nye County, Nevada: U.S. Geol. Survey Bull. 1294-E, p. E1-E12.
- Scott, R., 1966, Origin of chemical variations within ignimbrite cooling units: *Am. Jour. Sci.*, v. 264, p. 273-288.
- Stewart, J. H., and McKee, E. H., 1968, Geologic map of the Mount Callaghan quadrangle, Nevada: U.S. Geol. Survey Geol. Quad. Map GQ-730.
- 1970, Geologic map of Lander County, Nevada: U.S. Geol. Survey open-file map.
- Webb, A. W., and McDougall, I., 1967, A comparison of mineral and whole rock potassium-argon ages of Tertiary volcanics from central Queensland, Australia: *Earth and Planetary Sci. Letters*, v. 3, p. 41-47.

MANUSCRIPT RECEIVED BY THE SOCIETY AUGUST 12, 1971

REVISED MANUSCRIPT RECEIVED NOVEMBER 15, 1971

PUBLICATION AUTHORIZED BY THE DIRECTOR, U.S. GEOLOGICAL SURVEY